ELSEVIER

Colloids and Surfaces
A: Physicochemical and Engineering Aspects 89 (1994) 227–239

COLLOIDS AND SURFACES A

Diffusive growth of phase-separating domains near a surface: the effect of reduced dimensionality

Francisco E. Torres [a,*], Sandra M. Troian [b]

[a] *Xerox Research Centre of Canada, 2660 Speakman Dr., Mississauga, Ont. L5K 2L1, Canada*
[b] *Department of Chemical Engineering, Princeton University, Princeton, NJ 08544, USA*

Received 18 December 1993; accepted 23 December 1993

Abstract

Recent experiments on phase separation in quenched binary liquid mixtures confined between closely spaced quartz surfaces have uncovered that the growth of domains near the surfaces is considerably faster than the growth of domains in the bulk. While the domains in the bulk coarsen in time as $t^{1/3}$, those near the surfaces coarsen as t^{α}, where α ranges from about 1.1 to 1.5 depending on the quench depth. Though it has yet to be determined whether this accelerated growth corresponds to the domains containing the more wetting or less wetting phase, it seems clear that both surface forces and reduced dimensionality can affect growth near a surface. To focus on the effect of dimensionality, we have developed a simplified model for the two-dimensional growth of a wetting domain. The model describes the wetting domain as a circular disk which remains at constant thickness and is fed by the diffusion of species from a three-dimensional supersaturated mixture. Numerical solution of the diffusion equation reveals that the radius of the disk increases linearly in time when the concentration field surrounding the disk equilibrates faster than the disk grows. At long times, however, when the concentration field cannot equilibrate at the rate of disk growth, the disk radius increases exponentially in time. Including the effect of other disks competing for the bulk species, as well as loosening the restriction of constant thickness, will slow the exponential growth, but the transition from linear to faster-than-linear growth will still occur. We draw favorable comparison between our theoretical results and experimental findings for both the growth at small quenches and the transition from linear to faster growth.

Keywords: Phase separation; Spinodal decomposition; Wetting

1. Introduction

During the last 20 years, metallurgists have been intrigued with the possibility of predicting the growth rates and structure factors which are measured experimentally for phase-separating binary fluid mixtures quenched into the thermodynamically unstable regime. This regime is characterized by the region in phase space (c,T) for which $(\partial\mu/\partial c)_{T,p} < 0$, where c is the concentration of one of the species in the mixture, T is the temperature, p is the pressure and μ is the chemical potential. The time evolution of such an unstable system undergoing a temperature quench can be described by the decay of an unstable state into two distinct phases which evolve by diffusion into macroscopic domains. In contrast to the decay of metastable states, no activation energy is needed for an unstable state to begin phase-separating into two distinct phases, and any infinitesimally small, long-wavelength fluctuation in the concentration can initiate the decay. This type of phase separation is called spinodal decomposition.

* Corresponding author.

SSDI 0927-7757(94)02812-7

Transmission electron micrographs of many binary systems undergoing spinodal decomposition reveal a highly interconnected bicontinuous structure in the bulk. When this structure is probed by X-ray, light or neutron scattering, one typically finds a broad peak developing in $S(q,t)$, the scattering intensity. As time evolves, this peak sharpens at some wavevector which we denote $q_{max}(t)$, all the while increasing its magnitude while $q_{max}(t)$ shifts toward smaller values. This development of a narrow peak signals the evolution of a single characteristic length scale, $2\pi/q_{max}(t)$, associated with the distance between interfaces separating the two distinct phases. Equivalently, for equal volume fractions, this characteristic length scale reflects the typical size of the growing domains [1].

A significant body of work on both the structure factor and the kinetics of binary systems undergoing spinodal decomposition has developed since the first experimental observations. Comprehensive reviews were presented by Skripov and Skripov [2] and Gunton et al. [3]. Given the good agreement between theoretical predictions and experimental findings for the case of simple binary fluids in bulk, more recent work on spinodal decomposition has focused instead on either the behavior of macromolecular mixtures instead of simple fluids, or on the effect of confinement. Measurements of the phase separation process near the critical point are often hampered by the very fast dynamics in simple binary mixtures; many experiments have therefore been restricted to behavior at late stages or at shallow quenches. Polymeric blends offer the possibility of investigating the very early stages of phase separation since the dynamics are considerably slowed down. The effective diffusion constant for a polymer with N segments scales as $1/N^2$ times the diffusion constant for simple binary liquid mixtures [4]. Even for deep quenches, one can therefore conveniently study the early and intermediate stages of phase separation [5].

Experiments in which binary mixtures are confined between closely spaced walls are designed to probe the possible effects of nearby walls on the kinetics of phase separation. The walls can affect the dynamics in two ways — through surface forces which can enhance or retard the growth of domains and through the geometrical constraint preventing growth perpendicular to the solid surface. Cahn [6] originally analyzed the equilibrium situation for an unstable binary mixture phase-separating near a wall. He predicted that close to the critical point, one of the phases will preferentially wet the nearby wall with a macroscopic layer. Though this last stage prediction has been experimentally verified in a number of different systems, the early stages involving the kinetics of growth of this wetting layer have largely remained unexplored. Several interesting experiments have been conducted over the past few years to investigate precisely these effects of a nearby wall on the spinodal decomposition process. We discuss these particular experiments in more detail below since they are the benchmark for our theoretical work.

We are aware of at least three different experiments designed to isolate the effect of nearby surfaces on the process of spinodal decomposition [7–11]. The studies by Guenoun et al. [7] were the first to establish exponents different from 1/3 (early stages) or 1 (late stages) for the temporal growth of domains near a surface. Direct visual observations of the phase separation process, made possible by the fact that light is scattered by the interfaces perpendicular to the plane of the image, gives optical confirmation of a remarkable layering of anisotropic structures growing near the walls. These elongated domains appear between a thin wetting layer and the bulk and seem to contain a preponderance of the non-wetting phase. Guenoun et al. measured the average domain separation, both parallel and perpendicular to the surface, and converted to appropriately scaled wavelengths. By the time the elongated domains appear, the bulk domains are measured to be growing with an exponent close to unity. This is the expected exponent for the late stages of spinodal decomposition, during which the early diffusion-driven growth, characterized by a growth exponent of 1/3, gives way to hydrodynamic effects and growth by capillary flow. In this late-stage regime, it was reported that the domains parallel to the wall grow with an exponent of 0.64 ± 0.15, while those in the bulk undergo linear growth.

The next group of experiments along these lines was performed by Cumming and co-workers

[8–10]. In contrast to the slower than expected exponents measured by Guenoun et al., these later investigations revealed surprisingly fast growth of surface domains. The light scattering studies on both polymer blends [8] and binary fluid mixtures [9] have uncovered two peaks in the scattering intensity $S(q,t)$: one peak evolving very quickly at short times starting from $q_{max} = 6.8\ \mu m^{-1}$, and another slower peak evolving after 1000 s. Both peaks smoothly move toward smaller wavevectors in time, suggesting the growth of surface and bulk structures. Plotting these two peak positions, $q_{max}(t)$, as a function of time clearly shows that the growth of domains is governed by two different power laws. For mixtures at critical composition, the growth of domains in the bulk is controlled by the usual diffusion-driven dynamics, which lead to an average domain size that scales as $L_B(t) = 2\pi/q_{max}(t) \propto t^{1/3}$, where t is time. In contrast, the average domain size near the surface, L_S, scales as t^{α}, where α ranges from 1.1 to 1.5 as the quench depth increases. Since one cannot neatly separate the effects due to surface attraction or repulsion from the effects of dimensionality, the physical origin of the fast signal remains unclear. By the effects of dimensionality, we mean the differences that arise because growth along a surface is two-dimensional, whereas growth in a bulk liquid is generally three-dimensional.

Bodensohn and Goldburg [11] did experiments in which they observed isolated, straight channels of one phase connecting layers of that phase that had wetted two closely spaced glass plates. The dynamics that they measured differed from the results of both Guenoun et al. [7] and Wiltzius, Cumming and co-workers [8–10], which is not surprising because the morphology in their system was quite different. In this study we did not attempt to interpret the results of Bodensohn and Goldburg; rather, we aimed to develop a theory for the growth of domains on a single surface in the absence of channelling.

Two explanations have been proposed to explain the differences in the results reported by Guenoun et al. [7] and those reported by Wiltzius, Cumming and co-workers [8–10]. The discrepancy might arise from the fact that the latter experiments probed the surface growth at shorter reduced times (i.e. time rescaled by ξ^2/D, where ξ is the fluid correlation length and D is the mutual diffusion constant) than in the Guenoun et al. experiments. A different mechanism might be operable at longer times, leading to the slower surface growth observed by Guenoun et al. Another explanation for the discrepancy involves the limited data set collected manually from the video images taken by Guenoun et al. The published data for the surface wavevector, $q_{max}(t)$, seem to contain two slopes that have been averaged together. The suggestion proposed by Troian [12] is that a larger data set would have weighted the averaged surface exponent closer to $-3/2$ (the slope associated with physical coalescence of surface domains), bringing the earlier measured values in line with the later measurements of Guenoun et al. In either case, these two experiments, as well as those carried out in thin capillary tubes by Bodensohn and Goldburg [11], establish that a nearby surface can strongly influence the kinetics of spinodal decomposition.

One of us [12] has investigated the consequences of a model for which the fast signal corresponds to the growth of non-wetting domains trapped near the solid surface. By a combination of domain coalescence and enhanced diffusion due to the geometric constraint of growth near a wall, it was suggested that the exponent associated with the non-wetting domains near a surface can achieve values much higher than 1/3, up to values of 1.5, for very deep quenches. The argument presented in that work shows that coalescence of domains near a surface can effectively triple the exponent associated with individual domain growth, but it fails to be valid in the limit that the surface domains grow only in two dimensions. There is not yet enough experimental evidence to decide whether the domains giving rise to the fast signal are three-dimensional domains, with large aspect ratios whose volume can be characterized by one parameter only (e.g. the radius $R(t)$), or whether they are truly two-dimensional disks of constant thickness growing along a wall. Having explored the case of the diffusive growth of non-wetting, three-dimensional domains undergoing coalescence near a surface, we decided to investigate the consequences of a truly diffusive model in which the domains prefer the confining solid surface and assume a

disk-like configuration at that wall. Before discussing the model, we describe some preliminary experimental evidence which suggests that the growing domains may in fact remain disklike and only grow laterally, all the while maintaining a fixed thickness.

The morphology of domain growth during spinodal decomposition is known to become self-similar in time. This characteristic gives rise to the familiar dynamic scaling for bulk scattering data: when the scattered wavevectors, $q(t)$, are scaled by $q_{max}(t)$, the structure function assumes a universal shape, $F[q/q_{max}(t)]$, such that $S(q,t) \propto {q_{max}}^{-d}(t)F[q/q_{max}(t)]$, where d represents the dimensionality of the scattering structure [13,14]. This function F is called the Furukawa function and its form has been numerically evaluated for both dilute and concentrated mixtures. If one assumes that the growth process with walls present still preserves this characteristic of self-similarity for each of the two modes, then one should expect to find that $q_{max}(t)$ scales as $[S(q_{max},t)]^{-1/d}$ for each peak in the scattering data. Fig. 3 of Ref. [8] shows one such plot for a particular quench (the quench depth was not specified). The slower mode has a slope of $-1/3$, indicating three-dimensional scattering objects, while the faster mode has a slope of $-1/2$, presumably reflecting scattering from two-dimensional structures. One would need to repeat many such measurements to establish a robust correlation confirming that the fast mode derives from the growth of a two-dimensional structure, since the curve-fitting procedures used to extract $q_{max}(t)$ and $S(q_{max},t)$ involve five-parameter fits and are subject to interpretation. In particular, the curve-fitting procedure in the bulk assumes a Furukawa form for the function F, while the fast mode peak is apparently only fit with a Gaussian function [9].

Despite the lack of a definitive correlation between the fast mode and two-dimensional structures, it is educationally valuable to explore the diffusive growth of fixed-thickness disks near a surface. The goal of this study is to see whether a model consisting of a fixed-thickness disk growing in two dimensions (as matter diffuses in three dimensions from a supersaturated solution) can predict growth exponents larger than the usual 1/3 exponent characteristic of diffusive growth in the bulk. The 1/3 exponent is a signature of diffusive isotropic growth. Since the presence of a wall breaks any such isotropy, we expect to find larger exponents for the radial growth of the disks. The question we are posing, therefore, is "Can the effect of dimensionality (i.e. two-dimensional or three-dimensional growth) significantly increase the growth exponent associated with diffusion?".

2. An idealized model

To understand better the dynamics that occur during phase separation along a surface, we analyze an idealized model of the diffusive process. Our approximation of the real system seems to predict scaling exponents and relationships for the growth rates which are consistent with the experimental results described earlier. Our analysis therefore seems a useful first step in the development of a complete theory. We choose in this work to concentrate on the temporal scaling laws and therefore study only the appropriate transport equations. The physical chemistry affecting the growth process, and in particular the effect of surface forces on the phase separation, will be considered in later work.

Ignoring any cooperative effect between domains, we first focus on one wetting domain by considering an isolated circular disk resting on a surface and surrounded by a semi-infinite reservoir of the second phase. We assume that radial growth occurs while the disk remains at a fixed thickness. We expect that the thickness of the disk will be set by the net balance of attractive forces between the wetting domain, the surrounding liquid phase, and the solid surface. We implicitly assume that the spreading process is fast enough to allow the disk to maintain this constant thickness as matter diffuses to it, i.e. the details of the spreading process do not retard the growth by diffusion. In this sense, we refer to the growing domain as a wetting domain.

To model the diffusion of species in the binary mixture to the wetting disk, we assume that Fick's law with a constant diffusivity D suffices to describe the flux. The interactions between the liquid phases

and the surface alters the chemical potential gradients near the surface and thereby renders the real situation more complicated, but we nonetheless expect our simplified description to provide reasonable results for the scaling of the domain size with time. For simplicity, we treat the mass transport as if it were diffusion of only one component, even though the phase separation obviously involves two or more species. In their seminal study of phase separation in bulk liquids, Lifshitz and Slyozov proceeded similarly and still obtained meaningful results [15].

Since the disk thickness is constant, the concentration of the diffusing species directly outside the disk should be constant if the interface is at local thermodynamic equilibrium, which we expect to be true after distinct phases appear. Also, far from the disk, the concentration of the diffusing species should become constant. Consequently, the diffusion will be driven by the difference between the far-field concentration and the concentration directly outside the disk. This difference is the supersaturation, but it is the supersaturation for a wetting domain and therefore will not necessarily equal the bulk supersaturation.

Fig. 1 depicts the various elements of our model problem. We denote the radius of the disk by $R(t)$, the thickness by h, and the concentration by $\hat{c}$. Also, we show the r and z directions of the polar coordinate system positioned at the center of the disk. In the remainder of this article, we

$$\hat{c} = c_\infty \text{ at } |x| \to \infty$$

$$\frac{\partial c}{\partial t} = D\nabla^2 c$$

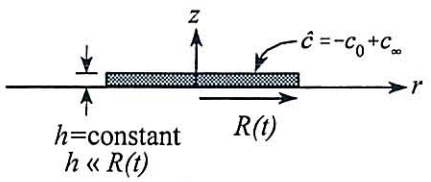

Fig. 1. Schematic diagram of a wetting disk growing radially along a macroscopic surface.

refer to the dimensionless concentration ($c = (\hat{c} - c_\infty)/(c_\infty - c_0)$ to simplify the analysis; we also have scaled all lengths with the initial radius $R_0 = R(t=0)$ and all times by R_0^2/D.

By assumption the dimensionless concentration c outside the disk satisfies the diffusion equation

$$\partial c/\partial t = \nabla^2 c \qquad 0 \leqslant z \leqslant \infty \qquad 0 \leqslant r \leqslant \infty \tag{1}$$

Note that Eq. (1) ignores the small thickness of the growing disk h. At the disk surface, which now corresponds to $z = 0$ and $0 \leqslant r \leqslant R(t)$, the concentration c equals -1, giving the boundary condition 1:

$$c = -1 \qquad \text{at } z = 0,\ 0 \leqslant r \leqslant R(t) \tag{2}$$

where $R(t)$ now refers to the dimensionless radius of the disk. Elsewhere along the surface the flux vanishes, yielding the boundary condition 2:

$$\partial c/\partial z = 0 \qquad \text{at } z = 0,\ r > R(t) \tag{3}$$

Far from the disk the concentration is uniform in our model, and the actual value of the far-field concentration merely acts as an additive constant. For convenience we therefore set the far-field dimensionless concentration to be zero by our choice of a dimensionless concentration, providing the boundary condition 3:

$$c = 0 \qquad \text{at } |x| \to \infty \tag{4}$$

We still need to specify the initial state of the system in order to calculate $c(x,t)$, the concentration at any point x and any time t. Since we are mainly interested in the behavior after the nucleation of the wetting phase, we do not expect the choice of an initial state to be crucial. Hence, we simply specify the concentration to equal the far-field value everywhere in space at time $t < 0$ (initial condition):

$$c = 0 \qquad \text{at } t < 0 \text{ and all } |x| \tag{5}$$

Eqs. (1)–(5) describe the spatial and temporal behavior of the concentration, given $R(t)$; consequently, a mass balance specifying $R(t)$ closes this set of equations. For a disk having an internal concentration c_d and a constant thickness h, the appropriate equation for the evolution of $R(t)$

assuming cylindrical symmetry is

$$2\pi R\frac{dR}{dt} = \Gamma 2\pi \int_0^R \frac{\partial c}{\partial z} r\, dr \tag{6}$$

The parameter Γ, defined by $\Gamma = (c_\infty - c_0)R_0/c_d h$, sets the magnitude of the dimensionless speed dR/dt. The left-hand side of Eq. (6) describes the increase in the mass of the disk as it grows, and the right-hand side describes the diffusive flux to the disk. To solve Eqs. (1)–(6) for $R(t)$ and $c(x,t)$, we performed boundary-element calculations. As discussed in the next section, the results compare rather well with the experimental data.

Despite favorable predictions for the disk growth rate using only a simple diffusive model, one should address the issue of collisions between growing disks because such collisions and the subsequent coalescence might produce significant enhancements in the growth rates, possibly resulting in a large change of the scaling for R as a function of t. This might happen because two disks that collide while growing on the surface would form a larger disk in much less time than either would have needed to form the larger disk in isolation.

We made a first attempt at predicting the role of collisions by numerically solving the following approximate balance for a population of colliding disks:

$$\frac{\partial \psi}{\partial t} + \frac{\partial}{\partial R}\left[\psi(R,t)\frac{dR}{dt}(R,t)\right] = \frac{1}{2}\int\int Q(R_1,R_2)\delta[R-(R_1^2+R_2^2)^{1/2}] \times \psi(R_1,t)\psi(R_2,t)\, dR_1\, dR_2 - \psi(R,t)\int Q(R,R_1)\psi(R_1,t)\, dR_1 \tag{7}$$

where

$$Q(R_1,R_2) = 2\pi(R_1+R_2)\left(\frac{dR_1}{dt}+\frac{dR_2}{dt}\right) \tag{8}$$

This population balance describes the evolution of $\psi(R,t)$, which is the probability distribution function quantifying the number of domains per unit area with radius falling between R and $R+dR$. The function δ is the Dirac delta function, and in Eq. (7) it serves to describe an instantaneous fusion of two disks with radii R_1 and R_2 into one larger disk with radius $(R_1^2+R_2^2)^{1/2}$ upon collision. The dR/dt terms represent the rate at which R increases as a function of R and t. The rate of collisions is approximated as $Q(R_1,R_2)\psi(R_1)\psi(R_2)$ where Q is given by Eq. (8), which ignores correlations between neighboring domains. By solving Eq. (7) for ψ, using the dR/dt results for an isolated disk, and calculating

$$\langle R\rangle = \int R_1\psi(R_1,t)\, dR_1 \tag{9}$$

as a function of time, we estimate the enhancement of the growth rates arising from collisions.

The next section summarizes our theoretical results for isolated disks, beginning with a scaling analysis and following with the numerical results. We then discuss our modeling of the rate enhancement arising from collisions. Favorable comparison is drawn between our predictions and recent experimental results, although future theoretical investigations are suggested to draw stronger comparisons.

3. Discussion of theoretical results

3.1. *Scaling behavior of* R(t)

Before presenting our numerical results, we discuss how one can understand the behavior of $R(t)$ by carefully studying the scaling behavior of Eqs. (1)–(6).

First, note that the choice of Eq. (5) as an initial condition causes the concentration gradients, and hence the flux, to be large near the disk at small times. However, this behavior is artificial in the sense that Eq. (5) does not represent the true physics of nucleation. If the disk radius does not change much over the times $0 \leqslant t \leqslant 1$, then this initial transient behavior is unimportant in our analysis of the growth at longer times because the concentration gradients will spread over a length scale comparable to the disk size by $t \approx 1$.

Consequently, the behavior at $t > 1$ will be independent of the activity at times $t < 1$. Since we are not trying to understand the short-time behavior in this study, we need only recognize that initial transients will exist but will disappear quickly except in cases for which the growth is very rapid.

Once the initial transients have died away, the concentration field will behave in a quasi-steady manner if the disk grows sufficiently slowly. In this regime, the concentration gradients can relax more quickly than the disk grows, which results in the concentration obeying

$$\nabla^2 c = 0 \tag{10}$$

Recall that the Green's function for Eq. (10) decays as ρ^{-1}, where ρ is the distance from a point source. Since the disk acts as a sink by incorporating matter from the surrounding phase as it grows, the concentration gradients near the disk will scale as $1/R(t)$ in this regime. From Eq. (6) it follows that the rate of change of $R(t)$ is constant, i.e.

$$\mathrm{d}R/\mathrm{d}t \propto \Gamma \tag{11}$$

Thus the disk radius grows linearly in time during the quasi-steady regime, which is very close to the growth observed by Shi et al. [9] at small quenches.

In order for the growth to be quasi-steady, the rate of change of c should satisfy the constraint

$$\frac{\partial c}{\partial t} \ll \frac{\Delta c}{R^2} \approx \frac{1}{R^2} \tag{12}$$

where Δc is the dimensionless concentration difference between the disk and the surrounding liquid far away. Our estimate for the magnitude of $\partial c/\partial t$ is

$$\frac{\partial c}{\partial t} \approx \frac{\Delta c}{R}\frac{\mathrm{d}R}{\mathrm{d}t} \approx \frac{1}{R}\frac{\mathrm{d}R}{\mathrm{d}t} \tag{13}$$

and with this estimate the restriction given by Eq. (12) becomes

$$R\frac{\mathrm{d}R}{\mathrm{d}t} \ll 1 \tag{14}$$

Together with Eq. (11), this constraint implies that the growth will be quasi-steady when $R \ll 1/\Gamma$, given that $t > 1$ also holds as required for the influence of the early transients to be negligible.

When $R(\mathrm{d}R/\mathrm{d}t)$ becomes comparable to unity, the concentration gradients should no longer be able to adjust faster than the wetting domains grow. In terms of dimensional quantities, this transition should occur when

$$R\frac{\mathrm{d}R}{\mathrm{d}t} \approx D \tag{15}$$

Thus we can test our theory by comparing measured values of $R(\mathrm{d}R/\mathrm{d}t)$ with reasonable estimates of the effective diffusivity D.

Once R becomes much larger than $1/\Gamma$, the radius increases much more quickly than the concentration gradients can relax due to diffusion. This causes the gradient $\partial c/\partial z$ in Eq. (6) to be approximately constant over the characteristic time scale for changes in R. Consequently, we expect exponential growth described by

$$R \approx \exp\left[\frac{1}{2}\Gamma\left(\frac{\partial c}{\partial z}\right)t\right] \tag{16}$$

In the work by Shi et al. [9] on guaiacol–glycerol–water mixtures, a transition from linear growth to faster growth is indeed reported, but exponential growth is not observed.

The idea of wetting domains growing exponentially in time when they accumulate matter solely from a diffusion process seems remarkable, but our analysis does suggest that exponential growth will occur if nothing else slows the spreading. Our original model does assume that the disk thickness remains constant, which means the disk instantaneously adjusts its radius as matter diffuses toward it. At some point, of course, the driving force for wetting cannot act that quickly, and the hydrodynamics of the wetting will cause the growth to be slower than Eq. (16) suggests. In the future we will investigate this aspect of the problem.

3.2. *Numerical analysis of the diffusion-limited growth*

To solve Eqs. (1)–(6) numerically and to verify the above statements about the behavior of $R(t)$, we developed a boundary element algorithm. The

formulation of the algorithm begins with the integral equation for $c(x,t)$ based on the Green's function for Eq. (1). This integral equation describes the concentration produced by point sinks distributed over a circle of radius $R(t)$, and when the flux is azimuthally symmetric, the integral equation becomes

$$c(x,t)=\frac{\sqrt{\pi}}{4}\int_{\tau=0}^{t}\int_{r_0=0}^{R(\tau)}F(r_0,\tau)\times\frac{\exp[-(r^2+r_0^2+z^2)/4(t-\tau)]}{(t-\tau)^{3/2}}\times I_0\left[\frac{rr_0}{2(t-\tau)}\right]r_0\,dr_0\,d\tau \tag{17}$$

The function $F(r_0,t)$ represents the cylindrically symmetric strength of the point sinks per unit area; in other words, it equals the dimensionless flux at the radius r_0 along the disk and at the time t. The scaling factor used to make F dimensionless is $\pi c_0 D/R_0$. Also, the function I_0 is a modified Bessel function [16]. As Eq. (17) states, the concentration at any point x and any time t depends on the value of the flux F at all locations on the disk and at all previous times, although the contribution from previous times becomes small as the time delay becomes large.

Upon defining the function $G(r,r_0,t,\tau)$ to be

$$G(r,r_0,t,\tau)=\frac{\exp[-(r^2+r_0^2)/4(t-\tau)]}{(t-\tau)^{3/2}}\times I_0\left[\frac{rr_0}{2(t-\tau)}\right]r_0 \tag{18}$$

one can write Eq. (17) at locations along the disk, where Eq. (3) holds, as

$$-1=\frac{\sqrt{\pi}}{4}\int_{\tau=0}^{t}\int_{r_0=0}^{R(\tau)}F(r_0,\tau)G(r,r_0,t,\tau)\,dr_0\,d\tau \tag{19}$$

Simultaneously solving Eqs. (6) and (19) for the functions F and $R(t)$ provides not only $R(t)$ but also the means to calculate $c(x,t)$.

In terms of F, Eq. (6) for dR/dt becomes

$$R\frac{dR}{dt}=-\frac{\pi}{2}\Gamma\int_{r_0=0}^{R(t)}F(r_0,t)r_0\,dr_0 \tag{20}$$

since the concentration gradient and the flux are related by the equation

$$\frac{\partial c}{\partial z}=\frac{\pi}{2}F \tag{21}$$

The factor of 2 arises because the disk only absorbs matter from the half space on one side of the surface; for a disk in infinite space, the gradients on either side of the disk at any given r would sum to πF.

We solve for the functions F and $R(t)$ which satisfy Eqs. (19) and (20) by discretizing the disk into elements and approximating F within each element. The elements are defined by

$$0\leqslant r\leqslant f_1R(\tau),\ f_1R(\tau)\leqslant r\leqslant f_2R(\tau),\ \ldots\ f_{N-1}R(\tau)\leqslant r\leqslant R(\tau) \tag{22}$$

where $0<f_1<f_2<\ldots<f_{N-1}$ are constants. These elements are circular rings. We choose $f_i=(i/N)^{1/2}$ in order to have elements with equal areas, but one can just as easily choose other discretizations.

Next, we approximate $F(r,\tau)$ as

$$F(r,\tau)=F_i(\tau)\qquad \text{for } f_{i-1}R(\tau)\leqslant r\leqslant f_iR(\tau) \tag{23}$$

where it is understood that $f_0=0$ and $f_N=1$, leaving N functions of τ to be determined. We further specify the functions $F_i(\tau)$ to be

$$\begin{aligned}&F_i(\tau)=e_{i1}\qquad \text{when } 0\leqslant\tau\leqslant\tau_1\\&F_i(\tau)=e_{ij}\theta_{j1}+e_{i,j-1}\theta_{j2}\qquad \text{when } \tau_{j-1}\leqslant\tau\leqslant\tau_j\end{aligned} \tag{24}$$

where e_{ij} are unknown constants and θ_{j1} and θ_{j2} are the functions

$$\theta_{j1}=1-\frac{\tau_{j-1}}{\tau} \tag{25}$$

and

$$\theta_{j2}=\left(\frac{\tau_{j-1}-\tau_{j-2}}{\tau_j-\tau_{j-1}}\right)\left(\frac{\tau_j}{\tau}-1\right) \tag{26}$$

Eqs. (24)–(26) give an approximation for $F_i(\tau)$ that

is continuous in τ, and the forms for θ_{j1} and θ_{j2} allow for the expected divergence at $\tau = 0$. Eqs. (25) and (26) also allow F to follow both the $F \propto 1/R \propto 1/\tau$ scaling expected during the quasi-steady period and the constant F scaling expected during the period of exponential growth.

With the above discretization, the problem reduces to specifying the number of elements N, choosing the time intervals defined by τ_j ($j = 1, 2, \ldots$), and solving for the constants e_{ij}. Since there are N different e_{ij} constants for each time interval $\tau_{j-1} < \tau < \tau_j$, we calculate these N values by requiring that Eq. (19) be exactly satisfied at the middle of each element when $t = \tau_j$. The numerical procedure consists of solving for e_{i1} by performing calculations for $t = \tau_1$, followed by successive calculations at $t = \tau_2, \tau_3, \ldots$ to determine $e_{i2}, e_{i3}, \ldots$ for $i = 1, 2, 3, \ldots N$. When solving Eq. (19) for e_{ij}, one must account for the singularities in $G(r,r_0,t,\tau)$, which we do by analytically removing the singularities before performing any numerical integrations.

Solving for the N values of e_{ij} at $t = \tau_j$ requires an iterative scheme because one does not know $R(t)$ for $\tau_{j-1} < t < \tau_j$ until one knows the values of e_{ij}. Thus, for each time interval we guess $R(t)$, calculate e_{ij} for $i = 1, \ldots N$, calculate a new guess of $R(t)$ from Eq. (20), and repeat the process until the e_{ij} values converge. Typically, the values converge in two or three iterations.

The boundary element algorithm described above does not require any specific choices for the times τ_j or the values of f_i, which is an important strength of the method. Although we did not experiment much with different choices for f_i, we did include in our code an automatic adjustment for the step size in τ. Without this adjustment, covering several orders of magnitude in $R(t)$ would require unreasonably large amounts of CPU time. At each time step, if the radius $R(t)$ did not change by more than a specified percentage, typically about 1%, then the time step was automatically doubled as long as it still satisfied $\Delta\tau < \tau_1 R^2(t)$. Likewise, if $R(t)$ increased too much, then $\Delta\tau$ was reduced by a factor of 2. As for the number of elements, we found acceptable convergence for $N \geqslant 10$. We implemented the above algorithm on a CRAY-XMP computer.

3.3. Numerical results

Figs. 2 and 3 illustrate the calculated behavior of $R(t)$ vs. t for the growth of a wetting disk when $\Gamma = 0.1$. Specifically, Fig. 2 shows the quasi-steady regime during which R increases linearly with respect to t; conversely, the plot of $\ln R$ vs. t in Fig. 3 clearly shows the exponential growth at

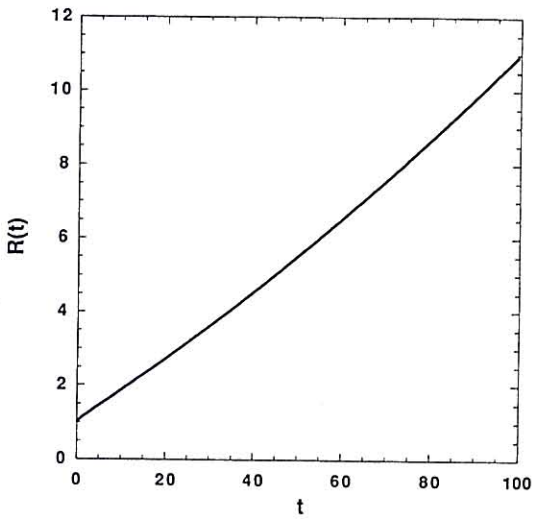

Fig. 2. Numerical results for $R(t)$ vs. t when $\Gamma = 0.1$.

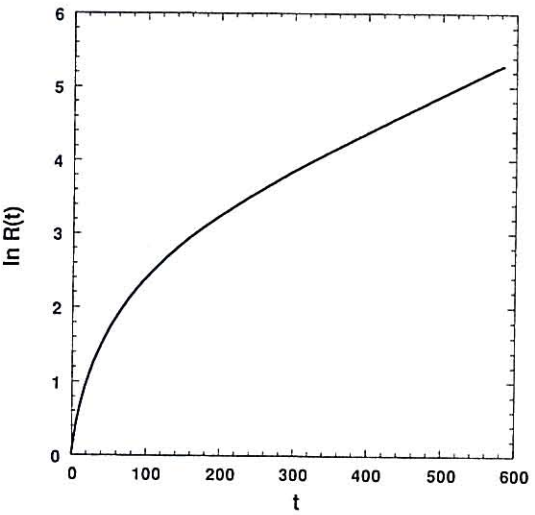

Fig. 3. Numerical results for $\ln R(t)$ vs. t when $\Gamma = 0.1$.

longer times. As expected, the initial transient dies away after short times, and the transition from linear to exponential growth occurs at $t \approx 100$. From Eqs. (11)–(14), the cross-over from linear to exponential growth should occur when $R(dR/dt) \approx 1$ or $t \propto \Gamma^2$. For the value of Γ chosen, we obtain excellent agreement with our scaling prediction. All the numerical results agree with our earlier scaling analysis of the behavior of $R(t)$.

Given the function F determined in the boundary-element calculations, one can calculate concentrations at any (x,t) by applying Eq. (17). Since the integrand is singular at the disk surface, calculations of $c(x,t)$ near the disk require special care in the evaluation of the associated integrals. As when solving for F, we analytically isolate the singularity before performing the integration to take care of this problem.

Fig. 4 is a plot of the concentration near the disk at $t = 1.0$. The figure illustrates c as a function of $z/R(t)$ for $r/R(t) = 0.1$, 0.5 and 0.95, where r is the radial coordinate in Fig. 1. Figs. 5 and 6 show similar plots for $t = 5.0$ and $t = 20.0$, at which times we expect the disk to undergo a quasi-steady growth. Comparison of these two figures reveals

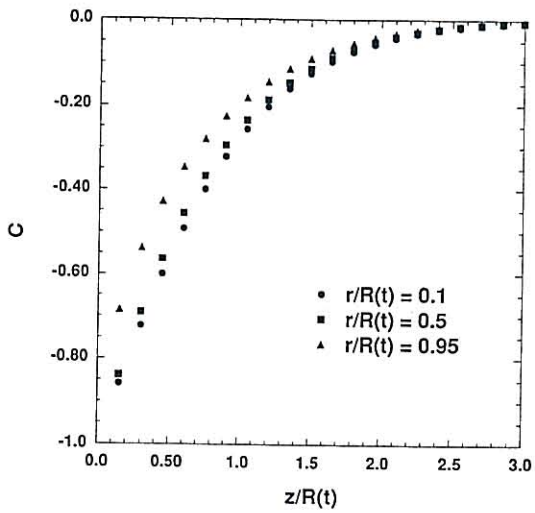

Fig. 4. Numerical results for the dimensionless concentration c vs. $z/R(t)$ at $t = 1.0$, when $\Gamma = 0.1$. The curves are for various radial positions: ●, $r/R(t) = 0.1$; ■, $r/R(t) = 0.5$; ▲, $r/R(t) = 0.95$.

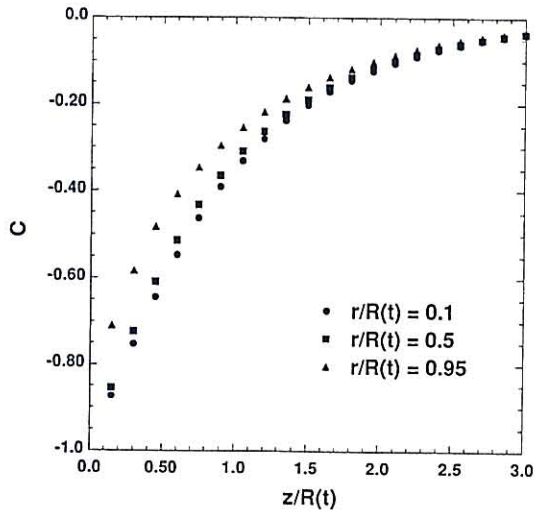

Fig. 5. Numerical results for the dimensionless concentration c vs. $z/R(t)$ at $t = 5.0$, when $\Gamma = 0.1$. The curves are for various radial positions: ●, $r/R(t) = 0.1$; ■, $r/R(t) = 0.5$; ▲, $r/R(t) = 0.95$.

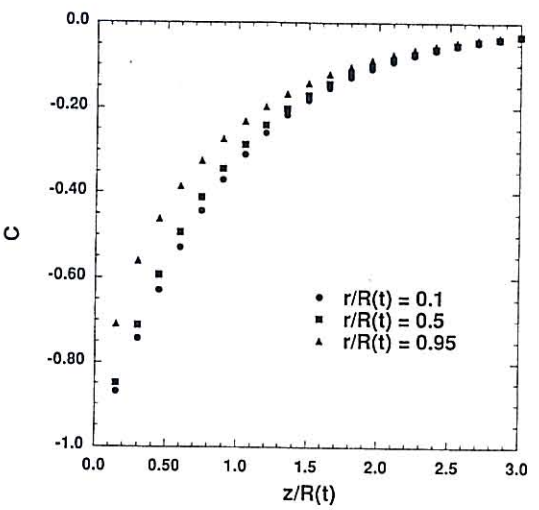

Fig. 6. Numerical results for the dimensionless concentration c vs. $z/R(t)$ at $t = 20.0$, when $\Gamma = 0.1$. The curves are for various radial positions: ●, $r/R(t) = 0.1$; ■, $r/R(t) = 0.5$; ▲, $r/R(t) = 0.95$.

the concentration curves at the different times for any one $r/R(t)$ to be nearly superimposable; therefore scaling lengths by $R(t)$ collapses the concen-

tration profiles for different times. This result is exactly what one should find during quasi-steady processes. The curves do not match those in Fig. 4 because the initial transient behavior still has some effect at $t = 1.0$.

Finally, Fig. 7 shows the concentrations at $t = 400$. The disk grows very rapidly at this time, and the concentration field cannot adjust at the same rate. Consequently, the concentration curves become increasingly steeper when plotted as a function of $z/R(t)$ because $R(t)$ becomes so large. The flux to the disk, $F(r,t)$, changes rapidly at small times but varies only slowly at $t > 200$, as Fig. 8 depicts for several values of $r/R(t)$. As discussed previously, the exponential growth at later times arises because $F(r,t)$ does not vary appreciably in time.

We also performed calculations for other values of Γ. In all cases, the results were consistent with the discussion above. For values of Γ larger than 0.1, the extent of the linear regime decreases, and when Γ is larger than about 0.5, one cannot distinguish a linear regime. Conversely, for values of Γ smaller than 0.1, the extent of the linear regime increases in the manner predicted by our scaling analysis.

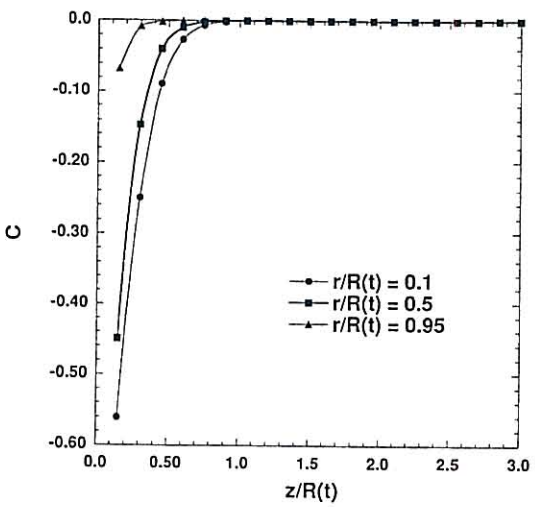

Fig. 7. Numerical results for the dimensionless concentration c vs. $z/R(t)$ at $t = 400.0$, when $\Gamma = 0.1$. The curves are for various radial positions: ●, $r/R(t) = 0.1$; ■, $r/R(t) = 0.5$; ▲, $r/R(t) = 0.95$. The lines connecting the points are a guide to the eye.

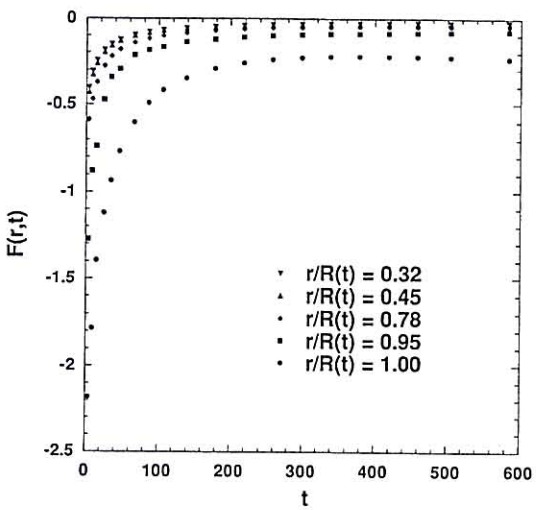

Fig. 8. Dimensionless flux $F(r,t)$ vs. t when $\Gamma = 0.1$. The curves from top to bottom are for $r/R(t) = 0.32$, 0.45, 0.78, 0.95 and 1.0.

3.4. Rate enhancement due to collisions

Using our results for dR/dt for an isolated disk, we now estimate the enhancement of the growth rate caused by collisions. To do this, we substitute dR/dt for isolated disks into Eq. (7), solve for ψ, and calculate $\langle R \rangle$ as a function of t. However, we only consider the linear growth regime because the exponential growth is already faster than the behavior observed in the experiments. For our purposes, we arbitrarily choose $dR/dt = 0.1$ for the single disk result to be used in Eq. (7).

Fig. 9 shows our results for the average radius $\langle R \rangle$ as a function of time. Interestingly, the growth appears to follow $R \propto t^{1.1}$, which is in excellent agreement with the experimental data reported by Shi et al. [9] for small quenches. Upon closer inspection, however, the actual behavior of R as a function of t does not strictly follow $R \propto t^{1.1}$. As Fig. 10 illustrates, the growth velocity actually approaches asymptotes at short and long times. At the short times, the areal coverage is small and collisions are infrequent, whereas at the longer times collisions occur quite often. It would be interesting to test whether the behavior depicted by Fig. 10 actually occurs in an experiment.

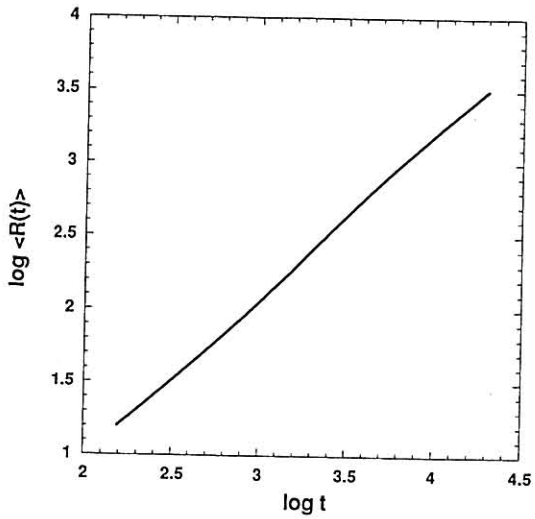

Fig. 9. Average domain radius $\langle R(t)\rangle$ as a function of time calculated using a population balance that includes the effects of collisions. The growth appears to follow $\langle R(t)\rangle \propto t^{1.1}$.

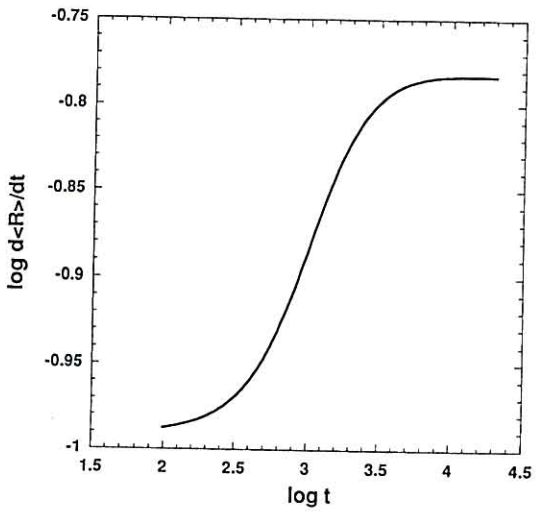

Fig. 10. Plotting the results in Fig. 9 as $\log(\mathrm{d}\langle R\rangle/\mathrm{d}t)$ vs. $\log t$.

Acquiring this experimental data might be difficult because $\mathrm{d}R/\mathrm{d}t$ is more difficult to measure accurately than R, and the predicted change in $\log(\mathrm{d}R/\mathrm{d}t)$ is not very large.

4. Comparison with experiment

Despite the approximations in our analysis, the results we obtained agree satisfactorily with published experimental results [8–10]. Our model predicts growth of two-dimensional wetting domains during phase separation that is much faster than the growth of domains in a bulk liquid, and in fact we actually predict what appears to be $R \propto t^{1.1}$ growth when the diffusion is quasi-steady and the disks undergo collisions. This behavior is precisely what Shi et al. [9] report for the growth at small quenches. Furthermore, video recordings of the experiments cited above confirm that collisions between surface domains do occur regularly.

At longer times or for deeper quenches, our theory predicts a transition to an even quicker growth mode, with the transition occurring when $R(\mathrm{d}R/\mathrm{d}t) \approx D$, R and $\mathrm{d}R/\mathrm{d}t$ being the unscaled radius and velocity, respectively, in this comparison. Based on the Wilke–Chang correlation suggested by Reid et al. [17] for calculating the diffusion constant in a dilute solution, we estimate a representative molecular diffusion for the experiments of Shi et al. to be $D = 4 \times 10^{-8}\ \mathrm{cm^2\ s^{-1}}$. As shown in Table 1, this value of D does indeed seem to correspond to the experimentally observed transition reported by Shi et al. Table 1 shows representative experimental values of $R(\mathrm{d}R/\mathrm{d}t)$ as a function of the measured exponent b in $R \propto t^b$ (see Ref. [9]), where we have used the equation

$$R = 2\pi/q \tag{27}$$

to estimate R from the reported wavenumbers q. As the growth changes from $R \propto t^{1.1}$ to $R \propto t^{1.5}$,

Table 1
Relationship between $R\,\mathrm{d}R/\mathrm{d}t$ and the kinetic exponent b

Quench (°C)	t (s)	$R\,\mathrm{d}R/\mathrm{d}t$ ($\mathrm{cm^2\ s^{-1}}$)	b
0.011	500	1.1×10^{-9}	1.08 ± 0.02
0.011	1600	4.4×10^{-9}	1.08 ± 0.02
0.041	100	4.3×10^{-9}	1.1 ± 0.02
0.041	440	2.5×10^{-8}	1.1 ± 0.02
0.126	17	8×10^{-9}	1.36 ± 0.06
0.126	78	1.1×10^{-7}	1.36 ± 0.06
0.219	23.5	7.7×10^{-8}	1.53 ± 0.08

the values of $R(dR/dt)$ do seem to change from being less than D to being equal to or greater than D.

Within the model and assumptions presented, we cannot yet explain the $R \propto t^{1.5}$ growth which is observed for the deeper quenches. Our results for diffusion-limited growth indicate instead that the length of two-dimensional wetting domains should grow exponentially in time. Although we have yet to resolve this difference, our results seem to suggest that some transport mechanism other than diffusion must become the growth-limiting step when the wetting domains are large and growing quickly. Our present view is that a likely rate-determining process during this late stage regime is the hydrodynamics of spreading, which is likely to be dominated by surface forces like van der Waals attraction. Further studies are needed to confirm this conjecture. Our results also suggest that the thickness does not remain constant at large times or for large quenches unless the growth is exponential, from which it follows that the two-dimensional scaling for the scattering should begin to degrade during the $t^{1.5}$ growth.

Acknowledgments

The authors are grateful to Andrew Cumming for many helpful discussions and for sharing videos of his experiments. Without his cooperation, this work would not have been possible.

References

[1] J.D. Gunton and M. Droz, Introduction to the Theory of Metastable and Unstable States, Vol. 183, Lecture Notes in Physics, Springer-Verlag, New York, 1983.
[2] V.P. Skripov and A.V. Skripov, Sov. Phys. Usp., 22 (1979) 389.
[3] J.D. Gunton, M. San Miguel and P.S. Sahni, in C. Domb and J.L. Lebowitz (Eds.), Phase Transitions and Critical Phenomena, Vol. 8, Academic Press, New York, 1983.
[4] P.G. de Gennes, J. Chem. Phys., 72 (1980) 4756.
[5] P. Wiltzius, F.S. Bates and W.R. Heffner, Phys. Rev. Lett., 60 (1988) 1538.
[6] J.W. Cahn, J. Chem. Phys., 66 (1977) 3667.
[7] P. Guenoun, D. Beysens and M. Robert, Phys. Rev. Lett., 65 (1990) 2406.
[8] P. Wiltzius and A. Cumming, Phys. Rev. Lett., 66 (1991) 3000.
[9] B.Q. Shi, C. Harrison and A. Cumming, Phys. Rev. Lett., 70 (1993) 206.
[10] A. Cumming, P. Wiltzius, F. Bates and J. Rosedale, Phys. Rev. A., 45 (1992) 885.
[11] J. Bodensohn and W.I. Goldburg, Phys. Rev. A, 46 (1992) 5084.
[12] S.M. Troian, Phys. Rev. Lett., 71 (1993) 1399.
[13] H. Furukawa, Phys. Rev. A., 23 (1981) 1535.
[14] K. Binder and D. Stauffer, Phys. Rev. Lett., 33 (1974) 1006.
H. Furukawa, Physica (Amsterdam), 123A (1984) 497.
[15] I.M. Lifshitz and V.V. Slyozov, J. Phys. Chem. Solids, 19 (1961) 35.
[16] I.S. Gradshteyn and I.M. Ryzhik, Table of Integrals, Series and Products (Corrected and Enlarged), Academic Press, New York, 1980.
[17] R.C. Reid, J.M. Prausnitz and T.K. Sherwood, The Properties of Gases and Liquids, 3rd edn., McGraw–Hill, New York, 1977.

C. R. Acad. Sci. Paris, t. 310, Série II, p. 1169-1173, 1990

Physique des surfaces et des interfaces/*Surface and Interface Physics*

Glissement à l'interface de deux polymères légèrement incompatibles

Françoise BROCHARD-WYART, Pierre-Gilles de GENNES et Sandra TROIAN

Résumé – Deux polymères A et B fondus ont une épaisseur d'interface $e=a\chi^{-1/2}$ où a est une taille moléculaire et χ le paramètre de Flory. Si il n'y a aucun enchevêtrement entre A et B, le frottement entre A et B est faible et de type Rouse – mais avec une viscosité $\eta_R(e)$ dépendant des échelles spatiales [1]. On peut en fait avoir quelques enchevêtrements, de probabilité $f=\exp(-N_e\chi)$ où N_e est la distance entre enchevêtrements dans A ou B massif [2]. Ils dominent la friction dès que $N_e\chi<\ln(N^3/N_e^{5/2})$, où N est le nombre de monomères par chaîne. Le régime de Rouse pourrait avoir des conséquences intéressantes en coextrusion.

Slippage at the interface between two slightly incompatible polymers

Abstract – *Two molten polymers* A *and* B *have a diffuse interface of thickness* $e=a\chi^{-1/2}$ (*where a is a monomer size and* χ *is the Flory parameter*). *If* A *and* B *are not entangled, we expect a weak Rouse friction – with a viscosity* $\eta_R(e)$ *which is size dependent* [1]. *We may also have some* AB *entanglements, with a probability* $f=\exp(-N_e\chi)$ (*where* N_e *is the number of monomers per entanglement in bulk* A *or* B) [2]. *The* AB *entanglements should suppress the slippage whenever* $N_e\chi>\ln(N^3/N_e^{5/2})$, *whete* N *is the degree of polymerisation. The Rouse regime might have some interesting rheological consequences for coextrusions.*

I. INTRODUCTION. – L'un de nous a discuté jadis le problème du glissement d'un polymère fondu sur une surface solide [3]. On attend un glissement facile si : (*a*) le polymère n'a pas de liaisons spécifiques avec la surface; (*b*) le polymère est bien fondu partout (pas de zone vitreuse ou cristallisée près de la surface); (*c*) la surface n'est pas trop rugueuse.

Expérimentalement, on n'observe souvent aucun glissement [4]. Toutefois, certaines observations dans une filière transparente [5] ou en rhéométrie plan/plan [6] suggérent un glissement, mais il n'est pas sûr que ces observations soient faites dans le régime de faibles contraintes ($\sigma\to 0$) qui était l'objectif de la référence [3]. Il se peut qu'une couche de polymère vitreux soit fréquemment présente près du solide.

Dans la présente Note, nous abordons un cas différent : celui de deux polymères fondus A et B, mis en contact le long d'un plan xy (*fig.* 1). Ces deux polymères sont en général incompatibles, avec un paramètre de Flory [7] $\chi>0$. L'épaisseur de l'interface AB est alors $e=a\chi^{-1/2}$ (où a est une taille de monomère) : e est indépendant des nombres de monomères par chaîne (N_A, N_B) pourvu que $N\gg 1$ [8].

Si χ est grand, il est clair que les chaînes A ne s'enchevêtrent pas avec les chaînes B, et on a donc la possibilité d'un glissement important. Ce problème a été abordé par Furukawa [9], mais sans apprécier pleinement le rôle relatif de la friction de Rouse (sans enchevêtrements) et de la reptation (avec enchevêtrements).

Nous reprenons cette discussion, au niveau des lois d'échelle, pour un cas simple et « symétrique » : les deux polymères A, B sont supposés avoir : (*a*) même longueur ($N_A=N_B=N$); (*b*) même distance entre enchevêtrements ($N_e\ll N$); (*c*) même viscosité $\eta_A=\eta_\beta=\eta$ en phase fondue, soit pour un modèle de reptation [10] :

$$\eta=\eta_1\frac{N^3}{N_e^2}\qquad (N>N_e) \tag{1}$$

Note présentée par Pierre-Gilles de GENNES.

0764-4450/90/03101169 $ 2.00 © Académie des Sciences

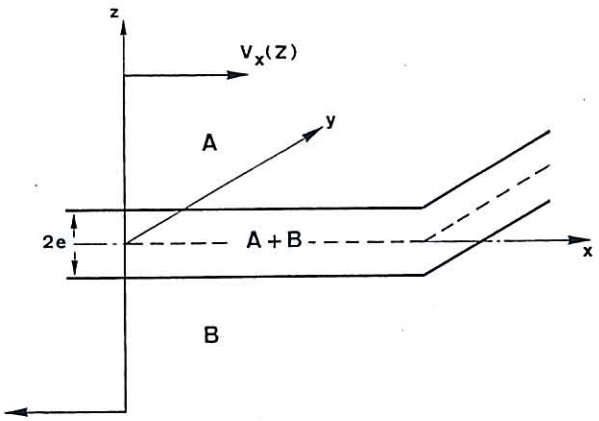

Fig. 1

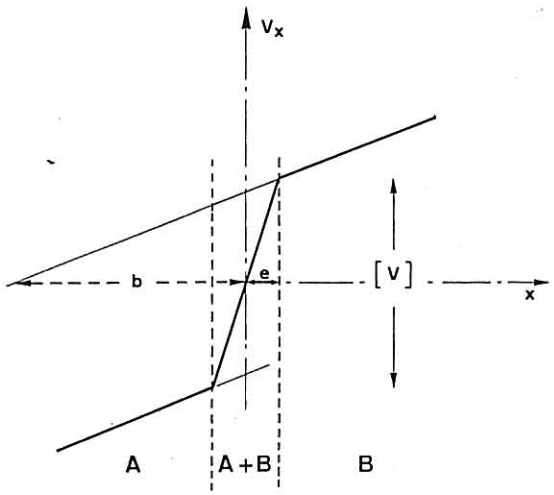

Fig. 2

Fig. 1. – L'interface entre deux polymères fondus (A et B), soumis à un champ de cisaillement simple $v_x(z)$.

Fig. 1. – The interface between two molten polymers (A *and* B), *under conditions of simple shear, with a velocity field* $v_x(z)$.

Fig. 2. – Profil de vitesse en glissement fort : le gradient est grand dans l'interface.

Fig. 2. – Velocity profile in conditions of strong slippage: the velocity gradient is steep in the interface.

où η_1 serait en gros la viscosité d'un fluide de monomères.

La probabilité f d'avoir un enchevêtrement AB dans l'interface a été analysée dans la référence [2] à propos de mesures d'adhésion (dont l'interprétation microscopique est plus délicate).

Le résultat central est :

$$f = \exp(-N_e \chi) \tag{2}$$

et montre que f décroît très vite quand N_e est grand.

II. LIMITE SANS ENCHEVÊTREMENTS. – Le profil de vitesse envisagé est représenté sur la figure 2. Dans la région interfaciale, on a un très fort gradient de vitesse $\sim[V]/(2e)$ et une faible viscosité de Rouse $\eta_R(e)$. Le produit viscosité × gradient est la contrainte de cisaillement σ, qui est la même partout :

$$\sigma = \eta \left.\frac{dv}{dz}\right|_{z>e} = \eta_R(e)\frac{[V]}{2e} \tag{3}$$

On peut exprimer le résultat (3) soit en termes d'un coefficient de friction de la jonction :

$$k = \frac{2\sigma}{[V]} = e^{-1}\eta_R(e) \tag{4}$$

soit en termes d'une longueur d'extrapolation (*fig.* 2) :

$$b = e\left(\frac{\eta}{\eta_R(e)} - 1\right) \cong e\frac{\eta}{\eta_R(e)} \tag{5}$$

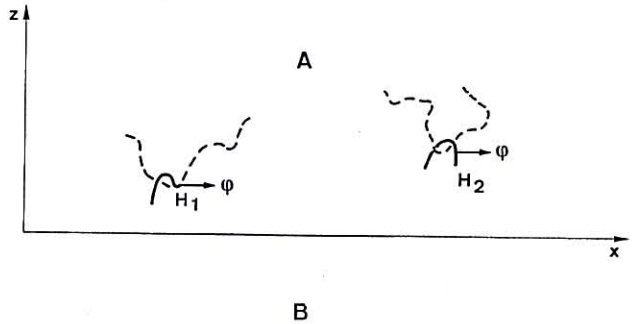

Fig. 3. – L'interface AB dans la limite d'enchevêtrement faible ($N_e\chi > 1$). Seulement quelques boucles issues de B (lignes continues) parviennent à ancrer des chaînes A (lignes pointillées).

Fig. 3. – Microscopic representation of the interface in the limit of weak entanglements ($N_e\chi > 1$): *only a few loops from* B (*continuous lines*) *can anchor certain* A *chains* (*dotted lines*).

Le point crucial est de définir la viscosité de Rouse $\eta_R(e)$ pour des échelles spatiales (e) inférieures à la taille d'une pelote. Un calcul direct de dissipation [1] montre que :

$$\eta_R(e) \cong \eta_1 \frac{e^2}{a^2} \qquad (e < R_0) \tag{6}$$

ce qui satisfait bien aux limites $e = a\,(\eta \to \eta_1)$ et $e = R_0 = N^{1/2} a\,(\eta \cong \eta_1 N)$.

En reportant l'équation (6) dans (4) et (5), on trouve un (faible) coefficient de friction – proportionnel à e – et une (grande) longueur d'extrapolation de Rouse

$$b_R \sim \frac{N^3}{N_e^2} \frac{a^2}{e} \sim \frac{a N^3}{N_e^2} \chi^{1/2} \tag{7}$$

Par exemple, si $\chi = 0{,}1$, $N = 10^3$, $N_e = 10^2$ et $a = 3\,A^2$, on attend $b_R = 10$ μm. Dans un cas de ce genre, la rhéologie d'une émulsion AB avec des gouttes plus petites que 10 μm peut être profondément modifiée.

III. Friction d'une jonction faiblement enchevêtrée. – Considérons le demi-espace occupé par l'un des polymères (A) (*fig.* 3). Il y règne une viscosité de système enchevêtré η. Il est important de réaliser que (contrairement aux viscosités de Rouse), la viscosité η est *la même à toutes les échelles* r, même pour $r < R_0 = N^{1/2} a$. En effet, on peut écrire η sous toutes la forme $\eta = \mu T_R$ où $\mu = kT/N_e a^3$ est un module de plateau (N_e = distance entre enchevêtrements) et T_R un temps de reptation des chaînes. Même si la perturbation mécanique qui agit sur les chaînes agit seulement sur une petite région r, les relaxations qu'elle entraîne impliquent toute la chaîne et le même temps T_R. En termes de vecteurs d'onde q :

$$\eta(q) \cong \eta(0) \qquad \left(\frac{1}{D} > q\right)$$

où $D = N_e^{1/2} a$ est la distance entre enchevêtrements [1].

A la surface de la région A sont placés des points d'ancrage de B avec une densité superficielle ν. Nous écrirons : $\nu = \nu_0 f$, où ν_0 est la densité de points d'ancrage (AA *ou* AB) dans une couche d'épaisseur D (si $D < e$), ou bien d'épaisseur e (si $D > e$). C'est surtout le domaine $e \sim D$ qui sera important dans la discussion. Alors, puisque le nombre

d'arcs enchevêtrés par centimètre cube est $\mu/kT=(N_e a^3)^{-1}$, on attend :

$$\nu_0=\frac{D}{N_e a^3}=\frac{1}{aD}$$

Sur chaque point d'ancrage, le milieu B exerce une force φ parallèle à Ox telle que $\nu\varphi=\sigma$.

Le champ de vitesses $v(z)$ résultant dans le milieu A satisfait à l'équation :

$$\eta\nabla^2 v+\nabla p=\varphi\sum_i \delta(\mathbf{r}-\mathbf{r}_i) \tag{8}$$

où la somme $\sum_i$ est étendue à tous les points d'ancrage. La pression p est telle que le polymère reste à densité constante (div $v=0$). La solution de (8) est une superposition de tenseurs d'Oseen :

$$\begin{cases} v_\alpha(\mathbf{r})=\sum_i \varphi_\beta T_{\alpha\beta}(\mathbf{r}-\mathbf{r}_i) \\ T_{\alpha\beta}(\mathbf{r})=\dfrac{1}{8\pi\eta r}\left[\delta_{\alpha\beta}+\dfrac{r_\alpha r_\beta}{r^2}\right] \end{cases} \tag{9}$$

A longue distance ($z>\nu^{-1/2}$), le champ de vitesses décrit un cisaillement uniforme $v_x=z\sigma/\eta$. A courte distance, à ce contact avec un site d'ancrage (i) de taille D, la vitesse (moyenne sur les orientations de $\mathbf{r}-\mathbf{r}_i$) vaut :

$$v\equiv\frac{1}{2}[V]=\frac{\varphi}{6\pi\eta D} \tag{10}$$

D'où un coefficient de friction :

$$k=\frac{\sigma}{(1/2)[V]}=(\text{Cte})\,\nu D\eta \tag{11}$$

IV. Discussion. – Le coefficient de friction total [déduit des équations (4) et (11)], a la forme :

$$\frac{2\sigma}{[V]}=k_{\text{total}}=\frac{\eta_1}{a\chi^{1/2}}\left[1+e^{-N_e\chi}\frac{N^3}{N_e^2}\chi^{1/2}\right] \tag{12}$$

On voit que, à $N_e\chi$ grand, le premier terme (friction de Rouse) l'emporte. Ceci reste vrai tant que :

$$N_e\chi>\ln(N^3 N_e^{-2}\chi^{1/2})\cong\ln(N^3 N_e^{-5/2})$$

Par exemple, avec $N=10^3$ et $N_e=10^2$, il faut $N_e\chi>10$, soit $\chi>0{,}1$.

Ces considérations peuvent jouer un rôle dans certains problèmes de *coextrusions*. Si $N_e\chi$ est en dessous de la valeur seuil, la longueur d'extrapolation est égale à b_R [équation (7)]. Cette longueur déduite de la faible friction de Rouse, est grande : si b_R devient supérieur à l'épaisseur des films de A, on n'aura plus de cisaillement dans ces films.

Note remise le 9 mars 1990, acceptée le 21 mars 1990.

Références bibliographiques

[1] F. Brochard-Wyart, 1978, non publié. *Voir* aussi (pour le cas enchevêtré) P.-G. de Gennes, *J. Physique*, 42, 1981, p. 473-477.

[2] P.-G. de Gennes, *C.R. Acad. Sci. Paris*, 308, série II, 1989, p. 1401-1403.

[3] P.-G. de Gennes, *C.R. Acad. Sci. Paris*, 288, série B, 1979, p. 219-220.

[4] J. MEISSNER, *Polymer testing*, 3, 1983, p. 291-301. *Ann. Rev. Fluid Mech.*, 17, 1985, p. 45-64.
[5] J. GALT et B. MAXWELL, *Modern plastics*, déc. 1964, McGraw Hill.
[6] R. BURTON, M. FOLKES, K. NARM et A. KELLER, *J. Materials Sci.*, 18, 1983, p. 315-320.
[7] P. FLORY, *Principles of polymer chemistry*, Cornell U.P., 1974.
[8] E. HELFAND, *Acc. Chem. Res.*, 8, 1975, p. 295-305. *J. Chim. Phys.*, 63, 1975, p. 2192-3001.
[9] H. FURUKAWA, *Phys. Rev.*, A40, 1989, p. 6403-6406.
[10] P.-G. de GENNES, *Scaling concepts in polymer physics*, Cornell U.P., 1985.

F. B.-W. : *Structures et Réactivités aux Interfaces, Université Paris-VI,*
11, *rue P.-et-M.-Curie*, 75005 *Paris;*
P.-G. de G. et S. T. : *Physique de la Matière condensée,*
Collège de France, 75231 *Paris Cedex* 05.